Photosynth Res (2013) 117:431–448
DOI 10.1007/s11120-013-9915-1

REGULAR PAPER

Thermal phase and excitonic connectivity in fluorescence induction

Agu Laisk · Vello Oja

Received: 8 March 2013 / Accepted: 19 August 2013 / Published online: 5 September 2013

Abstract Chl fluorescence induction (FI) was recorded in sunflower leaves pre-adapted to darkness or low preferentially PSI light, or inhibited by DCMU. For analysis the FI curves were plotted against the cumulative number of excitations quenched by PSII, n_q, calculated as the cumulative complementary area above the FI curve. In the +DCMU leaves n_q was <1 per PSII, suggesting pre-reduction of Q_A during the dark pre-exposure. A strongly sigmoidal FI curve was constructed by complementing (shifting) the recorded FI curves to $n_q = 1$ excitation per PSII. The full FI curve in +DCMU leaves was well fitted by a model assuming PSII antennae are excitonically connected in domains of four PSII. This result, obtained by gradually reducing Q_A in PSII with pre-blocked Q_B (by DCMU or PQH_2), differs from that obtained by gradually blocking the Q_B site (by increasing DCMU or PQH_2 level) in leaves during (quasi)steady-state e^- transport (Oja and Laisk, Photosynth Res 114, 15–28, 2012). Explanations are discussed. Donor side quenching was characterized by comparison of the total n_q in one and the same dark-adapted leaf, which apparently increased with increasing PFD during FI. An explanation for the donor side quenching is proposed, based on electron transfer from excited P680* to oxidized tyrosine Z ($TyrZ^{ox}$). At high PFDs the donor side quenching at the J inflection of FI is due mainly to photochemical quenching by $TyrZ^{ox}$. This quenching remains active for subsequent photons while TyrZ remains oxidized, following charge transfer to Q_A. During further induction this quenching disappears as soon as PQ and Q_A become reduced, charge separation becomes impossible and TyrZ is reduced by the water oxidizing complex.

A. Laisk (✉) · V. Oja
Institute of Molecular and Cell Biology, University of Tartu, Tartu, Estonia
e-mail: alaisk@ut.ee

Keywords Leaf · Fluorescence induction · Photosystem II · Electron transport

Abbreviations

a_{II}	Excitation partitioning to PSII
CA	Complementary area
Cyt	Cytochrome
DCMU	(3-(3,4-Dichlorophenyl)-1,1-dimethylurea
ETR	Electron transport rate
FI	Fluorescence induction
FRL	Far-red light
F_0, F_{in}, F_m	Fluorescence yields, minimum, initial, and final (maximum)
F_v	Fluorescence, variable
LED	Light-emitting diode
n_e, n_q	Number of PSII excitations, total and quenched
P680	PSII donor pigment complex
PC	Plastocyanin
P_{D1}	PSII donor pigment
PFD, PAD	Photon flux density, incident and absorbed
PQ, PQH_2	Plastoquinone, oxidized and reduced
PSII, PSI	Photosystems, II and I
Q_A, Q_B	Primary and secondary quinone acceptors in PSII
STF, SSTF	Single turnover flash, saturating
$TyrZ^{(ox)}$	Tyrosine Z (oxidized)
WOC	Water oxidizing complex

Foreword

My acquaintance with photosynthesis began with the book "Photosynthesis" by Rabinowitch and Govindjee (1969).

This book was a concise logical description of experiments and their interpretations, opening the door into the labyrinth of this basic natural process. Later I had the luck to cooperate with Govindjee on the book "Photosynthesis in silico", which we edited together with him and Lada Nedbal (Laisk et al. 2009). Then I learned to know him as a convinced skillful professional, exactly knowing—and saying—how a good book must be done. Later this valuable experience has helped me a lot in editing papers submitted to this journal. It is not too much to say that through the books he has edited Govindjee has been a teacher for at least two generations of photosynthesis researchers. We have dedicated the following investigation to Govindjee, as a part of the special issues on Photosynthesis Education, considering that chlorophyll fluorescence has been his favorite topic.

Agu Laisk

Introduction

Temporal induction of Chl fluorescence (FI) has been an important source of information for solidification of our understandings about PSII electron transport. Two recent thorough reviews (Stirbet and Govindjee 2012; Schansker et al. 2013) have been helpful in setting the stage for this study.

The basics of interpretation of the temporal fluorescence rise were laid out by two classics of photosynthesis research. The main idea of Duysens and Sweers (1963) was that the fluorescence yield increases as PSII reaction centers become closed, i.e., as Q_A becomes photochemically reduced under the influence of light. The relatively complex multiphasic OI(D)P transient induction curve was explained by cooperation of the two photosystems: PSII fluorescence rise is due to the net reduction of Q_A, but the inflections may be due to PSI, oxidizing Q_A via an intermediate electron carrier between the photosystems. This PSI effect ceases as soon as oxidized electron acceptors are exhausted, and fluorescence rises to its maximum P ($=F_m$) level; the interaction of PSI and PSII is thus responsible for the details of the OI(D)P transient.

The experimental basis of Duysens and Sweers was limited by low light intensities, due to the slow recorder and shutter responses. After Morin (1964) designed an ingenious fast-response fluorometer, additional inflections were resolved in the initial part of FI: at very high induction light, fluorescence rapidly approached a (presently denoted as J) level lower than the final F_m, approaching the F_m level more slowly, the rate depending on temperature. Based on this, Delosme (1967) stated that during the very initial, photochemical phase (the O–J rise), the quencher Q of Duysens and Sweers ($=Q_A$) is completely reduced, but fluorescence is still low due to the presence of a second hypothetical quencher, which is removed during the thermal phase while fluorescence is approaching F_m. A clear proof of this idea was the low fluorescence yield recorded after illumination with saturating single-turnover flashes (SSTF). Considering the extremely high light intensity of SSTF there is no doubt that Q_A is completely reduced (Joliot and Joliot 1979), but fluorescence yield stays only at 70–75 % of F_m. Joliot and Joliot (1964, 1977, 1979, 1981) considered a possibility that the second quencher may be located on the donor side, such that it would influence also the fluorescence transient of samples treated with DCMU (Joliot and Joliot 1977). They proposed a model (Joliot and Joliot 1977, 1979) that explained the results obtained at high light intensities by a double-hit process: Q_A is reduced after the first photon, and the oxidized primary PSII donor, $P680^+$, receives an electron from the secondary electron donor, TyrZ, in a short time compared to the duration of the flash; this would allow a second hit that would reoxidize P680 and reduce the hypothetical quencher Q_2.

During the last 35 years, researchers have attempted to find experimental support for this interpretation of the fast FI. The first detailed studies of the polyphasic fluorescence rise 20 years after the pioneering work of Delosme (1967) were published by Schreiber and co-workers (Schreiber 1986; Schreiber and Neubauer 1987; Neubauer and Schreiber 1987), who discovered that the thermal phase (I–P phase of Delosme) consists of two components, denoted I1–I2 and I2-P (Schreiber 1986), later called J–I and I–P (Strasser and Govindjee 1991). In this early work, various mechanisms causing quenching at the I1 and I2 levels were discussed. In the case of I1-quenching, a non-photochemical mechanism by oxidized PQ (static quenching) was ruled out, as this could be suppressed by DCMU (Neubauer and Schreiber 1987), however, quenching by Q_B remained a possibility. On the other hand, various pretreatments weakening the PSII donor side were shown to enhance I1-quenching (Schreiber and Neubauer 1987). Besides non-photochemical quenching by $P680^+$ in a special population of PSII, these authors also considered "dissipative photochemical quenching" involving recombination of the photochemically separated charges or a rapid cycle around PSII. Various hypothetical mechanisms have been proposed for the thermal phase, related either to the quencher R on the acceptor side (Delosme 1967), or to the quenchers Q_2 and D on the acceptor and donor side (Joliot and Joliot), or suggesting other non-photochemical processes enhancing the fluorescence yield (Samson and Bruce 1996). Stirbet and Govindjee (2012) summarize the major quencher candidates as follows: (1) $P680^+$ can quench Chl a fluorescence as efficiently as Q_A; (2) P680 triplet, $^3P680$, most likely $^3Chl_{D1}$ quenches in equilibrium with $^3P_{D1}$; (3) Carotene triplet ^3Car is an efficient quencher; (4) non-

photochemical quenching by oxidized PQ molecules; (5) reduced $Pheo_{D1}$ may be a quencher. The following two items were not included in the list: (6) Q_B-quenching by charge recombination from Q_B (Schreiber 2002) and (7) conformational changes influencing the fluorescence yield (Schansker et al. 2011).

In this work we propose another member to complete this list—quenching by TyrZ. This quencher was investigated by recording the number of photons quenched by PSII during the full FI curve at different light intensities. Considering the difference between the numbers of quenched photons and transferred electrons we suggest that oxidized TyrZ is the hypothetical quencher involved in the "double-hit process" of fluorescence quenching (Joliot and Joliot 1977, 1979). Quenching by $TyrZ^{ox}$ is photochemical, caused by cyclic charge transfer $P680^* \rightarrow TyrZ^{ox} \rightarrow P680^+ \rightarrow P680^*$.

Another controversial issue is excitonic connectivity. An understanding that PSII antennae are excitonically connected—making possible excitation transfer to an adjacent open center if the nearest reaction center happens to be closed by reduced Q_A—is based on the 1964 experiment by the Joliots, where *Chlorella* cells were illuminated by low light and the number of functional PSII centers was down-titrated by increasing concentrations of an inhibitor ortho-phenanthroline (Joliot and Joliot 1964, 2003). Relationship between the rate of O_2 evolution and the number of still active PSII centers was strongly nonlinear, indicating that the effective antenna size of an active center increased by about three times when adjacent centers were inhibited.

Recently we used another approach, gradually blocking PSII electron transport by PQ reduction during FI (Oja and Laisk 2012). Unexpectedly, we obtained linear relationships between the rate of PSII electron transport and the number of open PSII centers, indicating PSII units are excitonically disconnected. In the present work we analyze FI curves measured in intact sunflower leaves with and without DCMU, trying to throw more light on the above-described unsolved problems of PSII electron transport. Methodically our work distinguishes by careful quantification of the number of photons exciting PSII. Using the "cumulative complementary area" (Malkin and Kok 1966; Melis and Homann 1975; Paillotin 1976)—i.e., the number of photons quenched by PSII—as the independent variable (abscissa) for FI curves facilitates the quantitative mechanistic analysis of the transients. In agreement with earlier reports we recorded FI curves with variable sigmoidicity (rev. Stirbet 2013; Schansker et al. 2013), but after considering the dark pre-reduction of Q_A the strongly sigmoidal FI curves were well approximated by a model assuming four excitonically connected PSII in a domain. Reasons why blocking PSII electron transport from different sides results in different connectivity will be discussed.

Materials and methods

Plant growth conditions

Sunflower (*Helianthus annuus L.*) plants were grown in 4-l pots in nutrient-enriched soil in a growth chamber (AR-95HIL, Percival, from CLF Plant Climatics GmbH, Emersacker, Germany) at a PFD of 450 μmol quanta m^{-2} s^{-1}, 14/10 h day/night cycle, 25/20 °C temperature, 65 % relative humidity, and 380 ppm CO_2. Fully expanded, attached leaves of 3- to 4-week-old plants were used in experiments.

Measurement of fluorescence induction

In the laboratory-made two-channel leaf gas exchange measurement system (Fast-Est Instruments, Tartu, Estonia) the leaf was enclosed in a 32-mm diameter by 3-mm deep chamber and, at a flow rate of 0.5 mmol s^{-1}, flushed with 21 %, 2 % or 50 ppm O_2 and 200 ppm CO_2 in N_2, as indicated. Water jacket temperature was 22 °C and leaf temperature was close to it. The whole leaf chamber area was illuminated through a branched fiber-optic light guide. Plastic fibers (1 mm, Toray Polymer Optical Fiber, PF series, from Laser Components, Gröbenzell/München, Germany) were individually arranged in branches to produce uniform illumination of the adaxial leaf surface from several LED-based light sources. The actinic light causing fluorescence induction was simultaneously the fluorescence excitation light. Chlorophyll fluorescence emission was collected from the area of 2 cm^2 from the adaxial (upper) side of the leaf. The instrument system was controlled by an A/D and I/O board ADIO 1600 (Kontron, San Diego, CA) and a self-written Turbo Pascal program RECO.

Fluorescence induction was measured with the help of a PIN diode illuminated via the emission-collecting branch of fibers; the signal was further processed by a laboratory-made amplifier (Oja et al. 2010). The actinic (and exciting) light was produced by a LED-based source, connected with the illuminating branch of the fiber optics. Initially a 630 nm LED (ENFIS Ltd., UNO Tag Array) was used, which produced high-intensity light, but with a significant gradient of intensities across the leaf cross-section. In other experiments an amber LED (LZ4-00A100, LedEngin, 595 nm, 15 nm peak half-width) was used for inducing fluorescence, resulting in more uniform illumination across the leaf. The long-wave shoulder of both sources was cut off by short-pass filters FES 0650 (ThorLabs, Newton, NJ). At their maximum power the LEDs became heated up, causing a significant decrease in emission intensity (up to 20 % during 50 ms). To consider this, the excitation light intensity was recorded in parallel with fluorescence emission and the yield was calculated as the ratio of

fluorescence emission to excitation intensity. Long-wave fluorescence was sensed through an interference band-pass filter at 750 ± 20 nm (FB 750-40, ThorLabs) plus a red glass filter cutting at 650 nm. Parasite signals caused by cross-transparency of the exciting beam and by fluorescence of the plastic fibers were carefully measured and considered in data processing. The signal/noise ratio was very high—in figures inductions are presented without any averaging, as recorded data points joined by straight lines.

Long-wavelength light (720 nm) preferentially exciting PSI was used for pre-adaptation of leaves to low PSII light. The pre-conditioning light intensity was adjusted such that caused O_2 evolution (PSII ETR) of 5 μmol e^- m^{-2} s^{-1}.

Leaf absorptance spectrum was measured by spectroradiometer PC 2000 (Ocean Optic, Dunedin, FL) from a leaf disk placed in an integrating sphere and illuminated by a halogen bulb. For all light sources photon fluence rate absorbed by the leaf was calculated as the product of the spectra of the incident light and leaf absorptance.

PSI fluorescence

The PSI fluorescence component was measured using a deconvolution method that assumes any change in the spectral F_m/F_0 is caused by an invariant signal component—PSI fluorescence (Franck et al. 2002). The average F_m/F_0 was 7.9 between 675 and 685 nm but decreased steadily above 685 nm to an average value of about 5 beyond 720 nm. This pattern of change in F_m/F_0 is consistent with progressive appearance of invariant PSI fluorescence above 685 nm, establishing a basis for its calculation (Genty et al. 1990; Pfündel 1998; Peterson et al. 2001; Franck et al. 2002; Palombi et al. 2011). For sunflower leaves the average F_{PSI} was about 38 % of the average F_0 in the long-wave spectral window (730–770 nm). PSI fluorescence was subtracted from FI curves, where "PSII fluorescence" is indicated on the ordinate.

Photons exciting PSII and excitations quenched by PSII

The major methodical advancement in this work is calculation of excitations energetically active at PSII. In other words, it means calculation of excitations quenched by PSII and presentation of FI curves plotted against the cumulative number of such excitations. For these calculations, absorbed actinic PAD was found by integrating the product of incident light intensity and leaf absorption coefficient over the spectrum of the light source. The total pool of active PSII was measured as $4{\cdot}O_2$ evolution from SSTF applied on the leaf pre-adapted at low preferentially PSI light (Oja and Laisk 2000). Excitation partitioning ratio between PSII and PSI was assumed to be 2/3 and 1/3, respectively (see "Discussion" section). The number of photons exciting a single PSII was obtained by dividing the amount of photons absorbed by PSII, μmol m^{-2}, by the amount of PSII, μmol m^{-2}.

Initially the FI curves were recorded with respect to time, as usual. In Fig. 1 such an explanatory (theoretically constructed) FI curve is shown for incident PFD of 3,200 μmol m^{-2} s^{-1}. The FI curve was constructed exponential, as expected in the presence of DCMU without excitonic connectivity. Taking the typical values for leaf absorptance of 0.814 for the amber LED light at 590 nm, assuming excitation partitioning ratio to PSII, a_{II}, of 0.66 and a typical PSII density of 1.72 μmol m^{-2}, the rate of accumulation of PSII excitations (dose rate) was 1 ms^{-1}. Therefore, the abscissa units presenting the doze of PSII excitations, n_e, "occasionally" coincide for the time-related and excitation dose-related presentations. The shape of the recorded FI curve remains unchanged independent whether time-related or dose-related, but the latter presentation is convenient for the comparison of FI curves measured with different PFDs, because temporal differences in FI are canceled out.

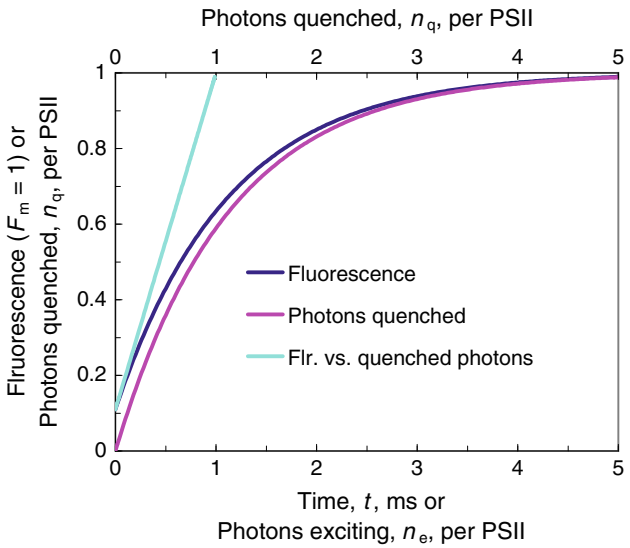

Fig. 1 Finding the number of photons quenched by PSII. An exponentially saturating FI curve was designed for a leaf, based on the following data: PFD = 3,200 μmol photons m^{-2} s^{-1}, amber (590 nm); leaf absorptance 0.814; excitation partitioning to PSII, $a_{II} = 0.66$; PSII density $N_{II} = 1.72$ μmol m^{-2}; PSII $F_0 = 0.11$; $F_m = 1.0$. *Black line* is the original recording, fluorescence F on the ordinate and time t on the abscissa. Next step, PSII excitation rate was calculated, which in the example was 1 ms^{-1}. Thus, the same (*black*) curve represents the dependence of fluorescence on the cumulative number of PSII excitations, n_e. Next, the number of photons quenched by PSII, n_q, was calculated as the "complementary area" above the fluorescence curve (see Fig. 2). With the given parameters the number of quenched photons n_q exponentially approaches one per PSII (*red line*). The straight (*turquoise*) line represents fluorescence plotted against photons quenched by PSII, n_q (*upper abscissa*)

In this work our final aim is to understand how photons interacting with PSII change the state of the photosystem. In this context only excitations quenched by PSII are important, because only these photons energetically interact with the core of the photosystem, but photons generating fluorescence leave their energy in the antenna mainly as heat. In order to find the cumulative number of quenched PSII excitations, n_q, at each point of the FI curve PSII excitations, n_e, were multiplied by the quenching coefficient $(F_m - F)/F_m$. The procedure is graphically illustrated in Fig. 2, where the quenching coefficient is the distance of F from F_m. Since the quenching coefficient gradually decreases with the increasing dose n_e, the fraction of quenched PSII excitations, n_q, counted from the beginning of the induction to a certain n_e value, equals to the "complementary area" between F_m and the rising $F(n_e)$ curve. For the assumed exponential fluorescence rise the fraction of quenched excitations decreases exponentially and the complementary area increases exponentially, approaching 1 photon quenched per PSII (Fig. 1).

Actually the photon doses were calculated considering also that LED emission rapidly decreased during the measurement of FI curves. For this also the incident light intensity was considered variable in parallel with the fluorescence yield, so that the PSII excitation dose

$$n_e(t) = \frac{a_{II}}{N_{II}} \int_0^t I(t')\mathrm{d}t' \quad (1)$$

and PSII quenched excitation dose

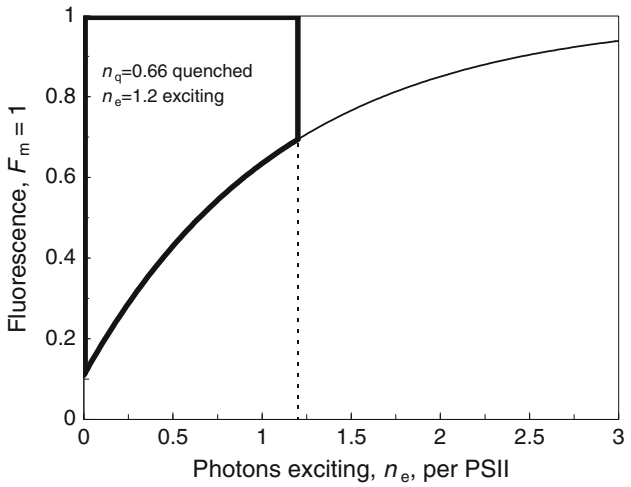

Fig. 2 Finding the number of photons quenched by PSII as the "complementary area" above the FI curve. Moving along the FI curve the complementary area initially increases rapidly (most photons are quenched), but becomes slower the closer the FI curve approaches F_m. The example area *box* shows, 1.2 photons had excited PSII, but only 0.66 were quenched. With the given parameters (legend to Fig. 1) the cumulative number of quenched photons, n_q, exponentially approaches 1 per PSII

$$n_q(t) = \frac{a_{II}}{N_{II}} \int_0^t I(t') \frac{F_m - F(t')}{F_m} \mathrm{d}t', \quad (2)$$

where $I(t')$ is photon absorption density (PAD, μmol m^{-2} s^{-1}) and $F(t')$ is fluorescence yield, both functions of time t' counted from the beginning of induction to the running value t, a_{II} is excitation partitioning ratio to PSII (0.66) and N_{II} is PSII density, μmol m^{-2}.

In order to see the effect of quenched photons on the state of PSII, the quenched dose, n_q, is plotted on the abscissa of the FI curve. This significantly changes the shape of the FI curve compared to the n_e or t based presentations, as n_q is a nonlinear function of t or n_e. The exponential case of Fig. 1 is a special one, where F and n_q both increase exponentially; therefore, their interrelationship is a straight line. Any distortion of the exponential relationship, e.g., due to excitonic connectivity, will be sensitively detected as bending the linear relationship towards concavity (Fig. 4). The example Fig. 1 represents the simple DCMU-inhibited case, where F approaches F_m as a result of one quenched excitation ($n_q \leq 1$)—meaning that the transfer of one electron turns a PSII into the F_m state. Below we use this same presentation also for uninhibited leaves, where several excitations are quenched before F approaches F_m. Exponential subsections of the FI curve and inflections between them will be clearly exposed in these "complementary area" presentations as well (Figs. 7, 10).

Results

Fluorescence induction in DCMU-inhibited leaves

Let us begin with a simple case, where electron transport is blocked by DCMU. In order to check the time course of inhibition, an introductory experiment was carried out with DCMU uptake under FRL. A sunflower leaf was cut and, with petiole in saturated water solution of DCMU, was exposed in the leaf chamber under 720 nm light. DCMU was absorbed by transpiration stream during a 3-h exposure (stomata remained open under FRL and in the dark in young sunflower leaves). Periodically steady-state O_2 evolution under FRL and saturating STF-induced O_2 evolution were measured with the aim of checking the degree of PSII inhibition. There was exact proportionality between the rate of steady-state O_2 evolution under the 720-nm excitation and the STF-induced O_2 evolution (Fig. 3). Dependent on the leaf, 85–95 % of PSII were inhibited at the end of the 3-h DCMU uptake.

In other leaves DCMU was taken up in the dark during 3 h, expecting a similar rate of inhibition as in the test

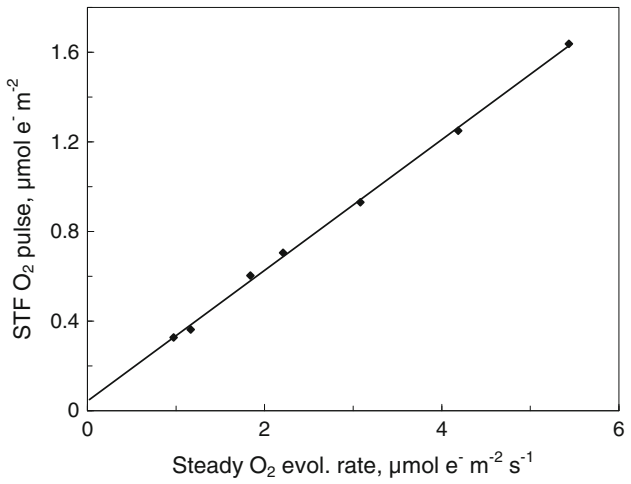

Fig. 3 Relationship between the steady-state PSII electron transport (under 695 nm, PFD of 135 μmol m^{-2} s^{-1}) and O_2 evolution from a saturating STF during gradual inhibition of PSII by DCMU taken up with transpiration stream

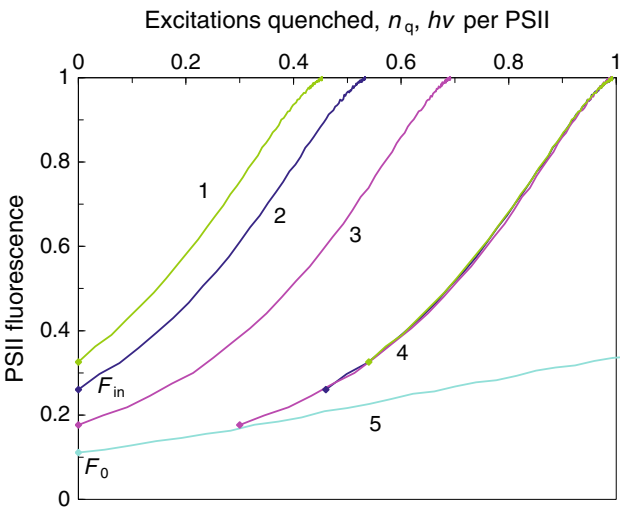

Fig. 4 Fluorescence induction in three DCMU-inhibited leaves (curves *1*, *2*, *3*) and the three curves shifted to the number of quenched excitations n_q of 1 per PSII (curve *4*). Curve *5* is the initial part of FI in an un-inhibited dark-adapted leaf. F_{in} is the initial fluorescence level. Inductions were measured under PFD of 3,000 μmol m^{-2} s^{-1} with amber LED, 2 % O_2, 200 ppm CO_2

experiment of Fig. 3. Fluorescence induction measured before the DCMU treatment displayed inflections and saturation characteristics typical of the dark-adapted leaves. To account for the finally un-inhibited fraction (maximum 15 %, typically less) we assumed that these PSIIs behaved the same as before the application of DCMU, subtracting their fractional contribution from the traces measured with maximally inhibited leaves (this assumption was probably sufficiently correct for the initial part of the induction, though the common PQ pool was probably reduced slower than with uninhibited PSIIs). The DCMU-inhibited F_m level was not lower than that of the non-inhibited leaf, but even slightly higher (Tóth et al. 2005). The small difference (<10 %) could be ascribed to changes in leaf optical properties during the long dark exposure with petiole in DCMU solution, increasing light scattering facilitating the emission of the long-wavelength component of Chl fluorescence.

In Fig. 4 the induction curves of three leaves are presented as functions of the increasing number of excitations quenched by an individual PSII. In this presentation the +DCMU inductions measured in different leaves were all sigmoidal, but to a different extent. Notably, the initial (F_{in}) level was higher than without the inhibition (F_0). Sigmoidicity tended to reciprocally correlate with the F_{in} value. In all +DCMU leaves the number of excitations quenched to reach the F_m state was significantly less than one per PSII, and the smaller the higher the F_{in}. This led us to the idea that the long dark exposure of the +DCMU leaves could cause some initial Q_A reduction, causing the increase of F_{in} and leading to the situation that less than one excitation had to be quenched in order to reach F_m. To test this hypothesis, the number of quenched excitations of individual curves was complemented to one per PSII by shifting the curves to the right. As a result of this the curves exactly merged (curves 4), though their starting points differed. The initial, offset part of the +DCMU FI curves could well be extrapolated to zero along the initial part of the curve measured before the uptake of DCMU (curve 5). This construction suggested that in the +DCMU experiments there was an initial Q_A reduction, different in individual leaves, but cutting off an initial part of the fluorescence induction. Without the preliminary Q_A reduction, the FI curves in the +DCMU leaves would have begun from the same F_0 as in the −DCMU leaves, approaching F_m via a strongly sigmoidal saturation process, similar in different leaves. The high F_m/F_0 value of 9 is characteristic for normally operating PSII (PSI fluorescence subtracted). Lower F_m/F_0 values likely indicate partial Q_A pre-reduction (non-photochemical quenching was avoided in these experiments).

Complete FI curves of the +DCMU leaves, offset to one excitation quenched per PSII, were compared to the model of connected PSII units (Fig. 5). The mathematical model of a connected PSII dimer (Oja and Laisk 2012) was numerically extended to four connected PSII (tetramer), which best fitted to the experimental curve (Appendix). The lake-type model of restricted connectivity (Paillotin 1976; Kramer et al. 2004) did not result in good global fit, but the initial (F_0) part required the *p*-parameter of 0.8 and the final (F_m) end of $p = 0.6$.

Dark-and light-adapted inductions

Most FI measurements have been carried out with dark-adapted objects with inhibited FNR, resulting in "dead-

end" inductions approaching F_m. In the dark-adapted leaves the acceptor side carriers of PSI are oxidized and the donor side carriers are reduced. The intrinsic PSII carriers Q_A and Q_B are generally assumed to be oxidized, but some reduction of the diffusible PQ pool is possible (Tóth et al. 2005, 2007). If the induction is started from a state pre-adapted at low light then S-states are randomized, Q_A is little reduced, but Q_B is randomized between Q_B and Q_B^- states. PQ pool is oxidized, as well as carriers around PSI, since in our experiments the pre-conditioning light was chosen to preferentially excite PSI. Thus, an anticipated difference between the light- and dark pre-adapted inductions is the finally established fast electron transport in the light-adapted state, contrary to the very slow electron transport rate in the dark-adapted state. Other differences are the initial S-state distribution (S_1 vs. randomized) and the initial reduction of Q_B (oxidized vs. randomized) and the possible partial reduction of the PQ pool. In this section we investigated, which kinetic differences in the FI curves could be related to the above-listed differences in the reduction states of the electron carriers.

Five different-aged leaves of the same sunflower plant were pre-adapted under 720 nm FRL producing PSII electron transport of 5 μmol e^- m^{-2} s^{-1}, but exciting PSI much faster. Thus, the inter-photosystem electron carriers were completely oxidized, in other aspects the preconditioning FRL was equivalent to a low PSII light. No non-photochemical quenching of fluorescence was induced under FRL. Fluorescence induction was initiated by changing the actinic light from FRL to the red LED providing 8,300 μmol photons m^{-2} s^{-1}. The initial parts of the low light-adapted FI curves were similar in all leaves, starting at $F_{in} = 0.15$ F_m (in FI started from low light the initial fluorescence F_{in} was always slightly higher than the true F_0) with the initial slope potentially spanning from F_0 to F_m per 6 PSII photons (Fig. 6). All light-adapted curves J-inflected to slowly increasing fluorescence at $F = 0.3F_m$ after about one photon was absorbed per PSII.

Now the same leaves were dark-adapted for 10 min and FI was measured again with the same light intensity as before. The dark-adapted FI curves differed significantly from the light-adapted curves, but, contrary to the light-adapted ones, the dark-adapted curves also differed between individual leaves of the same sunflower plant. The initial dark-adapted F_0 value scattered. In all cases the very initial slope of the FI curve was somewhat higher than that in the light-adapted state, but the slope sigmoidally increased as soon as on average 0.5 photons were absorbed per PSII. This sigmoidicity was different in different leaves, but the maximum slope was about two times steeper than the initial slope. Different from the light-adapted FI, the dark-adapted FI curves rapidly reached a high level of fluorescence of 0.5–0.8 F_m at the J inflection after about one photon was absorbed per PSII.

At closer inspection the initial rapidly rising sigmoidal phase of FI curves in dark-adapted leaves (Fig. 6) resembles those in partially DCMU-inhibited leaves. This suggests that reduced PQ could accumulate during the dark exposure, occupying a part of the Q_B sites similarly to DCMU. This hypothesis was tested by a dark exposure in anaerobic atmosphere, known to increase the reduction potential in leaf cells and chloroplasts. In the leaf dark-adapted in 21 and 2 % O_2 the initial slope of the FI curve

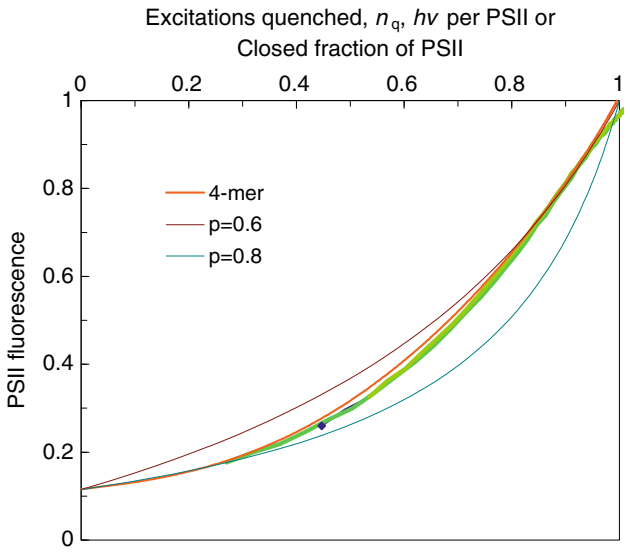

Fig. 5 Curve 4 from Fig. 4 (*green*) approximated by the model of four excitonically connected PSII in a domain (4-mer, see Appendix) and by the model of (Paillotin 1976) with different p values

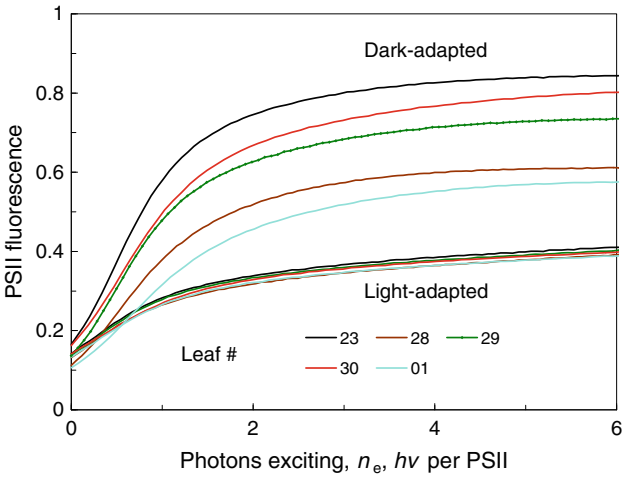

Fig. 6 Fluorescence inductions in four sunflower five leaves pre-adapted in the dark or under FRL of 720 nm, 230 μmol m^{-2} s^{-1}, supporting PSII electron transport of 5 μmol m^{-2} s^{-1}. Induction was measured under PFD of 8,300 μmol m^{-2} $s^{-1}$with the 630 nm LED. Recorded data points are shown on one curve (*dark green*), other curves are plotted as straight lines connecting the data points. Leaf numbering is arbitrary

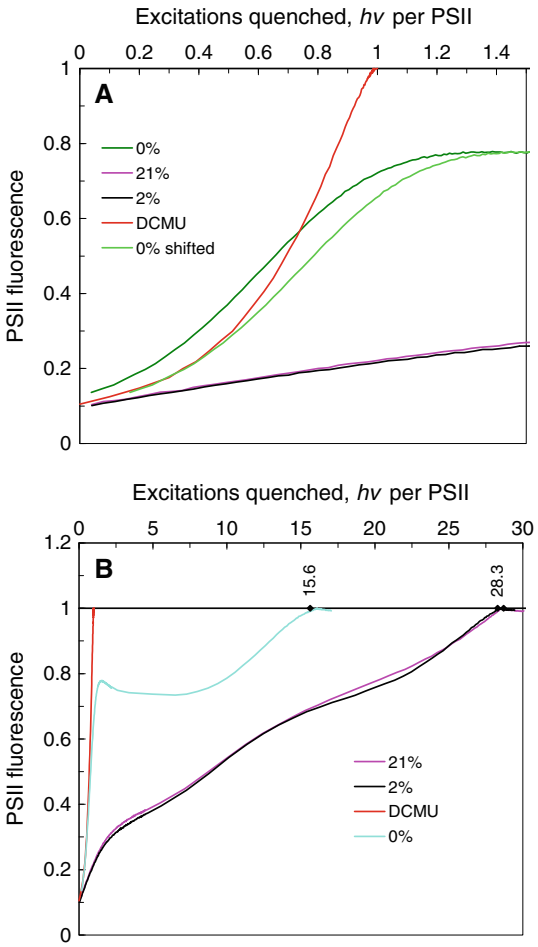

Fig. 7 Fluorescence induction under 3,000 µmol m^{-2} s^{-1}, amber LED, in leaves dark-adapted for 10 min under different O_2 concentrations (indicated in the legend). **A** Initial parts. Fluorescence induction in anaerobiosis (0 % O_2) was shifted to coincide with the induction curve measured in a DCMU-inhibited leaf. **B** Full induction; the number of quenched excitations is indicated above the *horizontal line*

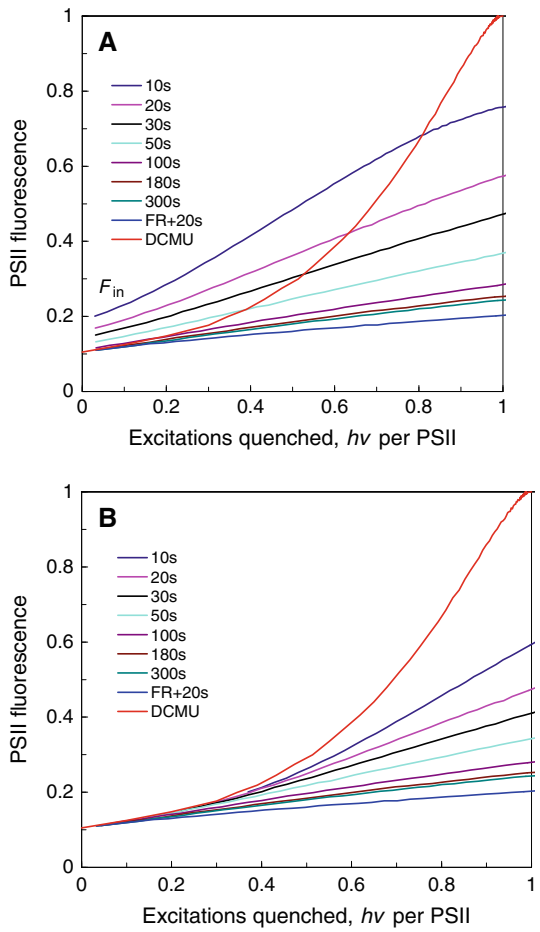

Fig. 8 Two fluorescence induction curves were measured under PFD of 3,000 µmol m^{-2} s^{-1}, amber LED, with dark intervals of different length between the two (indicated in the legend). **A** Initial parts of the second induction are shown in comparison with a +DCMU induction curve. **B** Induction curves shifted to complement one another (see text)

was very low, but after dark adaptation in the absence of O_2 the initial fluorescence level was higher, as well as the slope increased sigmoidally (Fig. 7A). After an offset to the right by 0.17 excitations per PSII the initial part of the anaerobic FI curve merged with that of the +DCMU curve. Thus, as expected, dark adaptation in anaerobiosis causes pre-reduction of Q_A by 17 %, but closure of a large part of Q_B—as indicated by the high J inflection level and significantly smaller total dose of quenched PSII excitations, decreased by 13 excitations per PSII compared to the aerobic curves (Fig. 7B).

This section of the study was completed by experiments where the diffusible PQH_2 pool was varied over a wide scale. A full FI curve was run with a dark-adapted leaf, which rather completely reduced the ET chain. After a dark exposure of different length another FI curve was run, which started from the redox state of electron carriers as relaxed from the initial complete reduction during the dark exposure. After the shortest, 10 s dark exposure, Q_A had oxidized to the extent which caused rather low initial fluorescence F_{in} of about 2 F_0 (Fig. 8A). Nevertheless, the FI curve still rose rapidly to the J inflection at about 0.8 F_m. After longer dark exposures the F_{in} level decreased, as well as decreased the height of the J inflection.

The kinetic behavior of these briefly dark-adapted FI curves is reminiscent of the DCMU-inhibited curves. In the DCMU experiments we shifted the curves to the number of quenched excitations of one per PSII, resulting in a FI curve beginning from the completely oxidized Q_A. Here the curves are only partially resembling the DCMU experiments, because of incomplete Q_B occupation more than one excitation may be quenched for complete Q_A reduction. Nevertheless, we assumed that the initial parts of the curves actually form one unique FI curve, except that they were started at different Q_A pre-reduction levels, causing different

F_{in} levels. Based on this assumption, each of the curve with higher F_{in} was shifted to the right to meet the same fluorescence value on the curve with the next lower F_{in}. As a result of this a boundary curve was formed which coincided with the initial part of the curves from +DCMU leaves (Fig. 8B). The result encouraged us to conclude that during dark adaptation the Q_A reduction level dropped faster than the Q_B occupation by PQH_2, suggesting either redox equilibration of Q_A with the PQH_2 pool with a high equilibrium constant, or direct oxidation of reduced Q_A by an external electron acceptor (e.g., O_2). When light was turned on again after the dark interval, the re-induction required just one excitation quenched per PSII to reach the J inflection, where Q_A reduction again became equal to, or just slightly higher than, the fractional occupation of Q_B by PQH_2.

Figure 9 shows full inductions from the same measurements. As an example, instead of fluorescence, Q_A reduction state is plotted on the ordinate, calculated from fluorescence using the connected tetramer model of Fig. 5 as a nonlinear ruler relating fluorescence to the Q_A reduction. The number of excitations quenched by PSII during the whole induction is plotted on the abscissa. This number increased from 19 to 34 e^- per PSII as the dark exposure lengthened from 10 to 300 s. This change indicates that the number of excitations quenched by PSII could very likely be equal to the number of electrons transferred through PSII in this experiment. Assuming that only PQ oxidation was responsible for the increasing electron capacity of the transport chain from 19.0 to 33.9, we get the estimated higher limit of 15 e^- per PSII or 7.5 PQH_2 molecules per PSII. However, in the next section we see that the number of quenched excitations actually overestimates PSII electron transport at high light intensities.

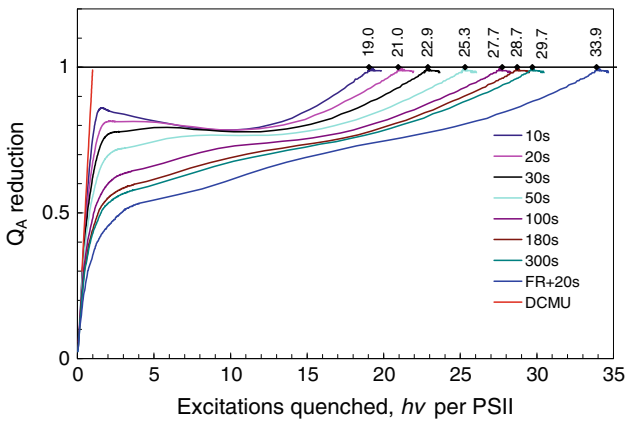

Fig. 9 Induction curves of Fig. 8 presented in full length. Q_A reduction state was calculated from fluorescence level using the connected tetramer model as a nonlinear ruler relating Q_A reduction to the fluorescence level. Figures above the *horizontal line* represent the full n_q (apparent electron capacity) of the electron transport chain, based on Chl fluorescence quenching

Donor side quenching

Neglecting the donor side quenching—which potentially may be of non-photochemical character—the number of PSII quenched excitations equals to the number of PSII charge separations, necessary to reduce the electron transport chain (e.g. Figs. 7B, 9). At high light intensities, however, the PSII donor side induces an additional false component into the fluorescence quenching, not related to electron flow through PSII. Therefore, one can anticipate that inductions with one and the same leaf, repeated under different light intensities, will reveal the number of quenched excitations, which will be larger the higher the light intensity.

In order to check this hypothesis, one and the same leaf was repeatedly dark-adapted and FI was measured using different actinic light intensities. Recorded FI traces are plotted with respect to the cumulative number of quenched excitations in Fig. 10. At the lowest PFD of 250 μmol m^{-2} s^{-1} the whole ET chain became reduced after 19 excitations were quenched per PSII, but the higher the PFD the greater was the calculated number of quenched excitations. In order to keep the number of quenched excitations constant (as the capacity of ETC is expected to be constant in one and the same leaf, the closest to that measured with the lowest PFD of 250 μmol m^{-2} s^{-1}), the light intensity had to be multiplied by a PSII efficiency coefficient as indicated in the panel.

The result shows that high light intensities are significantly less efficient in PSII electron transport than calculated from fluorescence quenching, evidently due to the donor side quenching of fluorescence, not coupled with

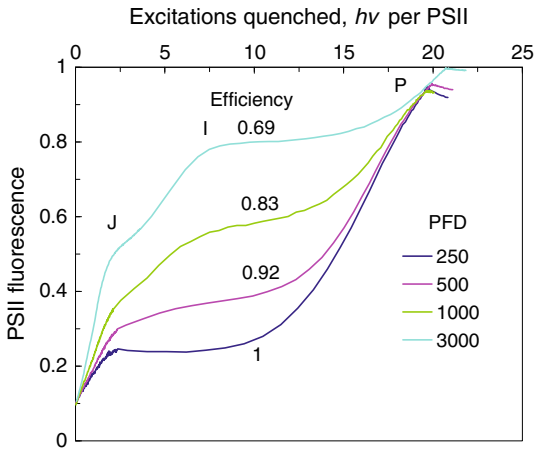

Fig. 10 Fluorescence inductions were measured in one and the same leaf under different light intensities (as indicated, μmol m^{-2} s^{-1}) after repeated dark adaptations. Under PFD of 250 μmol m^{-2} s^{-1} the full number of quenched excitations n_q was 19 per PSII. At higher PFDs the calculated n_q was bigger. Efficiency coefficients at the curves indicate, which part of the photons had to be considered active in PSII electron transport in order to obtain the constant total number of 19 excitations quenched per PSII

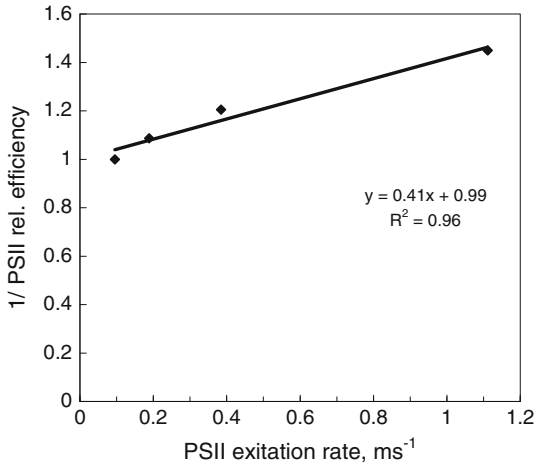

Fig. 11 Reciprocal of PSII efficiency (from Fig. 10) plotted against the PSII excitation rate. The slope of the *trend-line* indicates the dead time of 0.41 ms, during which PSII is blocked for electron transport after a successful electron transfer

electron transfer to Q_A. Following Joliot and Joliot (1977) it is clear that if a photon hits a PSII with reduced TyrZ and P680 and oxidized Q_A, then Q_A becomes reduced and TyrZ remains oxidized for as long as determined by the time of S-state advancement. If one assumes that subsequent photons hitting the PSII with TyrZ oxidized and Q_A reduced are "donor side quenched" and thus inefficient for electron transport, then PSII may be considered a photon counter, similar to the Geiger–Müller type counter of nuclear particles. In this device after each successful count a "dead time" follows, during which the photons are ignored.

The rate of counting (=rate of charge transfer to Q_A, n) by this sort of photon counter is hyperbolically related to the rate of photon arrival, n_0, as follows

$$n = \frac{n_0}{1 + n_0\tau}, \tag{3}$$

where τ is the dead time. The Q_A reduction efficiency

$$\frac{n}{n_0} = \frac{1}{1 + n_0\tau} \text{ or reciprocally } \frac{n_0}{n} = 1 + n_0\tau. \tag{4}$$

Thus, the reciprocal of the Q_A reduction efficiency is linearly related to the rate of photon arrival, the slope indicating the dead time τ. The corresponding plot of our data (Fig. 11) indicates the average dead time of 0.41 ms—the time after a successful charge transfer to Q_A, during which the photons are donor side quenched without an accompanying Q_A reduction.

Discussion

As described in Introduction, in this work we revisited the fluorescence induction process with an aim to throw light on the old controversy between the Q_A model of Duysens and Sweers (1963) and the thermal phase model of Delosme (1967), trying to find an answer to the question, what are the photochemical and thermal phases and how are they related to the Q_A reduction?

Methodical advances

As emphasized in the Methods section, this work is novel in its quantification of photon flux exciting PSII and photon flux quenched by PSII. The measurements of incident photon fluxes (PFD) were carried out with a calibrated spectro-radiometer. The spectral extinction coefficient of the leaf was measured in an integrating sphere and the absorbed PAD was calculated by multiplying the spectra of the incident PFD and leaf absorptance. The so-found PAD was multiplied by the excitation partitioning ratio, to find the photon flux rate exciting PSII. Presentation of FI curves as functions of the number of PSII excitations retains the characteristic time-dependent shape of the curve, but makes them independent of the excitation light intensity. Instead of referring to the characteristic inflections happening at certain time of t ms, the inflections take place after a certain number n_e of PSII excitations independent of excitation intensity. Due to these advances we were finally able to calculate the cumulative number of photons quenched by PSII—i.e., the photons whose energy could become available for charge separation and transfer in PSII.

Along with the precise quantification of absorbed photons, two parameters are critical in this analysis—the area density of PSII centers and the partitioning of excitations between PSII and PSI in the leaf. PSII density was determined as $4{\cdot}O_2$ evolution from SSTF applied on a leaf pre-adapted to a low, preferentially PSI light (Chow et al. 1991; Oja and Laisk 2000). Considering that at 720 nm about 6 % of absorbed photons excite PSII, but the rest excite PSI (Pettai et al. 2005), we used the 720 nm FRL source for pre-adaptation to low light, applying an intensity resulting in linear ETR ($4{\cdot}O_2$ evolution rate) of 5 μmol e^- m^{-2} s^{-1}. Though pre-adaptation under FRL has been reported to cause some specific phenomena (Schansker and Strasser 2005), these were not noticeable in our experiments, but only those interpretable to be caused by a low PSII and relatively stronger PSI light—mainly due to the complete oxidation of PQ. The preconditioning FRL was always turned off immediately before the actinic light was turned on. Typically the integral O_2 evolution pulse in response to an individual SSTF was between 0.25 and 0.5 μmol O_2 m^{-2}, correspondingly the PSII density was estimated to be between 1 and 2 μmol m^{-2}. Miss factor was neglected, considering that in the $S_3 \rightarrow S_0$ transition it is only 3 %, though may be significant in the $S_2 \rightarrow S_3$ transition (Han et al. 2012). The

only problem with this method of determination of PSII density is the assumption of equal distribution of S-states during steady-state photosynthesis. If the slowest, S_3 state would accumulate in steady-state, the multiplication of O_2 evolution by four could over-estimate the actual PSII density. In this case the axis of quenched excitations could be over-stretched in Fig. 4, to the extent that curve 3 could integrate to 1 excitation per PSII. However, in this case the increased F_0 of this curve would remain unexplained, so we do not question our PSII density values.

The excitation partitioning factor (or the relative optical cross-section of PSII), a_{II}, was assumed to be 0.66. Usually this factor is assumed to be 0.5, but evidence indicates the distribution of excitation in favor of PSII (Strasser and Butler 1977; Canaani and Malkin 1984). Recently relative excitation capture spectra of PSII and PSI were measured in pigment-protein complexes purified from chloroplasts of cucumber leaves grown under light of different spectral composition. Excitation partitioning a_{II} [=PSII/(PSI + PSII)] varied between 0.58 and 0.73 for sunlight-grown leaves, with the most likely values being between 0.6 and 0.65 (Hogewoning et al. 2012).

Using PSII density determined from SSTF O_2 evolution and excitation partitioning factor $a_{II} = 0.66$ we calculated the actual PSII excitation rate, s^{-1}, and the cumulative number of quenched excitations, i.e., the cumulative number of PSII charge separations during FI. In these procedures random experimental errors were very small, but the above-discussed systematic (interpretation) problems could lead to some overestimation of the quenched excitation scale. Therefore, it is not impossible that the best-fit number of four connected PSII is somewhat overestimated, though it is in agreement with some earlier reports (next section). Nevertheless, the proposed method could be an introduction to further connectivity analyses, presently retarded due to widely scattering results, caused by neglecting the dark pre-reduction of Q_A.

Excitonic connectivity between PSII

The first indication about PSII connectivity was obtained in an experiment, where PSII centers were gradually inhibited in *Chlorella* suspension and a nonlinear relationship was obtained between the rate of O_2 evolution and the number of functional PSII centers (Joliot and Joliot 1964). In the present work we made a similar measurement of the rate of steady-state O_2 evolution and the SSTF-determined number of functional PSII centers during the uptake of DCMU by transpiration stream in a sunflower leaf. The obtained relationship between the number of active PSII and steady-state O_2 evolution rate was linear (Fig. 3). An explanation is the difference of experimental objects. If a sunflower leaf would take up eosin red by transpiration stream, the leaf would not become colored absolutely uniformly, but by contrasting spots between the conducting veins on the leaf blade. If DCMU was taken up similarly to eosin, the inhibition occurred not by individual PSII inside an excitonically connected domain, but by groups of many connected domains in a spot. The overall result would be similar to gradual reduction of the operating leaf area, inevitably producing proportional relationships between area-based parameters.

However, the spotty character of PSII closure by DCMU seems to be deeper in the structure of the photosynthetic machinery than veins and stomata. In another series of measurements we closed PSII not by an inhibitor, but by gradually increasing PQ reduction, either in steady-state dependent on light intensity or during low–high light induction starting with all open and ending with mostly closed PSII (Oja and Laisk 2012). In these transients the rate of O_2 evolution was also linearly related to the number of open PSII, thus suggesting there is no excitonic connectivity between PSII antennae.

Generally speaking, linear relationships were obtained between the (quasi)steady-state rate of O_2 evolution and SSTF-induced O_2 evolution in measurements, where light was continuously present, but PSII centers were gradually closed by blocking the Q_B site either by PQH_2 or by DCMU (Oja and Laisk 2012). Contrary to these, a sigmoidal relationship was obtained in the present and other works when initially Q_B sites were pre-blocked either by DCMU or PQH_2 in the dark, but Q_A was gradually reduced by illumination during the subsequent FI curve. A solution to the dilemma could be a model, where domains containing several PSII centers are feeding electrons to a relatively isolated PQ pool. Across such domains about four PSII seem to be excitonically connected, but their output is common, such that the whole domain is simultaneously blocked by DCMU of PQH_2 (Joliot and Joliot 1992, 2002; Lavergne et al. 1992; Joliot et al. 1992). On the other hand, as discussed by Stirbet (2013), sigmoidal FI traces could be caused not by excitonic connectivity at all, but by dependence of electron donation on S-states and prolonged electron transfer time from pheophytin to Q_A due to the gradually increasing transmembrane electric field during the transient (Vredenberg 2008; Vredenberg et al. 2009), which could even induce conformational changes leading to gradually increasing fluorescence yield (Schansker et al. 2013). In this case the nonlinear dependencies are expected only during the dark–light induction, but not when light is continuously present and the quinone pool is gradually getting reduced—exactly as measured.

Reported widely variable values of the connectivity parameters seem to indicate highly dynamic flexible organization of the connected antenna system (Haferkamp et al. 2010). On the other hand, such variability needs to be

reconciled with the contemporary information about the obligatorily stable dimeric structure of PSII (Hankamer et al. 1995) with a defined $C_2S_2M_2$ coarse-grained antenna system (Broess et al. 2006), suggesting relatively constant excitonic connectivity (Broess et al. 2008; Cafarri et al. 2011). In this work we suggest a reason for the apparent variability of excitonic connectivity—neglecting the pre-reduction of PSII acceptor side carriers before the FI measurement.

A clearly contradictory result was obtained in DCMU-inhibited leaves, where fluorescence approached F_m far before one charge separation had occurred in PSII. Since this is impossible in principle, we assumed that Q_A was partially pre-reduced, due to which the initial part of FI was truncated. On this basis we shifted the curves recorded in different leaves to $n_q = 1$ excitation quenched per PSII, where the initially different FI curves merged, forming completed sections of one and the same FI curve. Without this the formal connectivity parameter—calculated from different sections of the FI curves—would have been significantly different in leaves of one and the same plant.

The so-revealed complete sigmoidal induction was well fitted by the model of a connected tetramer (Appendix)—an extension of the dimer model (Oja and Laisk 2012), based on the general connected domain model (Den Hollander et al. 1983). Introducing a mathematical basic parameter—probability p of excitation transfer from a closed center to another open center—Joliot and Joliot (1964) derived theoretical expressions for the dependence of the fluorescence yield and the photochemical yield on the fraction of open RCs. The approach of the Joliots has been further elaborated for more convenient experimental determination of the fitting parameters (Paillotin 1976; Strasser and Stirbet 2001; Strasser et al. 2004; Stirbet 2013), but the basic assumption of limited excitation transfer probability has remained. Our connected tetramer model assumes a joint antenna for all four monomers, from where excitation is harvested by the reaction centers with certain rate constants operating in parallel. Fluorescence remains at the lowest, F_0 level for as long as all centers are open, but the level increases as 1, 2, or 3 centers become closed. This process explains the very low initial slope of the FI curve (Fig. 4). The maximum level F_m is reached as soon as all four monomers are closed by Q_A reduction. The tetramer model globally fits the whole FI curve, while the Joliot approach requires that p be decreased from 0.8 to 0.6 over the whole FI (Fig. 5). Our result is in good agreement with the early evidence that energy transfer occurs in a domain of 3–5 connected PSII units (Joliot et al. 1973).

The model (Appendix) assumes every quenched photon causes electron transfer to Q_A, which, in the light of the donor side quenching (see below) seems not to be completely true at the high light intensity of 3,000 μmol m^{-2} s^{-1}. However, below we see that the rate constant of excitation capture by electron transfer from P680* to $TyrZ^{ox}$ is still about ten times slower than the rate constant for excitation capture by electron transfer from P680* to Q_A, which means that if a photon hits a domain where TyrZ is oxidized at one PSII, the excitation will preferably be quenched by Q_A reduction in another center, but not by donor side quenching due to $TyrZ^{ox}$ reduction. In addition to this, in the +DCMU experiments the dominant S-state step is from S_1 to S_2, which is the fastest of all steps, leaving very little chance for the second photon to hit a PSII with oxidized TyrZ. Therefore, neglecting the donor side quenching in the model of connected PSII introduces only an insignificant error.

Strong re-binding of PQH_2 to the Q_B site

In intact organisms such as leaves and algae respiratory metabolism is accompanied by an increase in the reductive potential of the cell medium, sufficient to cause partial pre-reduction of Q_A in the dark (Tóth et al. 2007), as it happened during anaerobiosis in this work (Fig. 7). Such inexplicit pre-reduction of Q_A cuts off the initial, strongly sigmoidal part of FI recordings. The recorded parts of the curves begin from different initial fluorescence levels F_{in} higher than F_0, and with different initial slopes dependent on which part of the sigmoidal curve the FI recording begins. Neglecting such Q_A pre-reduction in the dark leads to underestimation of excitonic connectivity, as discussed in the previous section, and to misinterpretation of the initial slopes of FI curves. Expressed in relation to PSII photons the initial slope of the FI curve is very low, pointing on F_m after 5–6 photons excited PSII. Its mechanistic meaning is the decrease of the effective rate constant of excitation capture from the connected antenna due to the closure of one PSII in the tetramer domain, as explained above. Expressed with respect to time the initial slope still continuously increases with increasing light intensity, up to 200,000 μmol quanta m^{-2} s^{-1} (Kobližek et al. 2001).

Pre-reduction of the PSII quinone electron carriers in the dark suggests some similarity between DCMU and PQH_2 in blocking the Q_B site. A general notion is PQH_2 is released from the Q_B site and replaced by PQ, inexplicitly assuming that PQ has a higher binding constant than PQH_2. The third, Q_B-less state was suggested (Robinson and Crofts 1983), a logically necessary intermediate state during the quinone exchange process. The continuous exchange of PQ and PQH_2 between the binding site and the diffusible pool occurs repeatedly, as typical of a binding site of an enzyme—in fact PSII is water-PQ reductase, for which PQ is the substrate and PQH_2 is the competing product. The fractional time of the Q_B site occupation by

PQ and PQH_2 depends on the concentrations and binding constants (affinities) of the quinone species.

In a recent work we analyzed the product inhibition of PSII by PQH_2, measuring the rate of O_2 evolution during an induction process reducing the bound and diffusible quinone carriers at the PSII acceptor side (Oja et al. 2011). The plot of the rate of PSII electron flow against the pool size of PQH_2 was a straight line starting at the maximum PSII throughput rate of 0.5 e^- ms^{-1} at completely oxidized PQ and approaching zero at the full reduction of PQ. We concluded that—similarly to an earlier work carried out on isolated chloroplasts (Robinson and Crofts 1983)—in intact leaves PQH_2 is a strong product inhibitor for PSII, competing with PQ for the Q_B site with about equal binding constants.

The pathway of electrons reducing the inter-photosystem carriers in the dark is not completely clear. A preferable candidate for this function is the chloroplastic NDH, reducing PQ at the expense of NADPH (Sazanov et al. 1998; Jans et al. 2008). In this case pre-reduction of Q_A is possible via the $Q_A \leftrightarrow PQH_2$ redox equilibrium, such that when 94 % of the PQ pool is reduced, Q_A is reduced in about 19 % of the reaction centers (Tóth et al. 2007). Oxidation of pre-reduced PQH_2 is a slow process, catalyzed probably by plastid terminal oxidase (Rumeau et al. 2007; Laureau et al. 2013) or reversibly via NDH as soon as NADPH reduction level decreases. For interpretation of FI it is important that after both, Q_A and PQ were reduced during preceding illumination, Q_A reduction level rapidly drops in the dark, though PQH_2 still remains reduced. If FI is repeated before PQH_2 has been oxidized, the kinetics are like those of the DCMU-inhibited leaves, sigmoidally approaching the J inflection (which now is close to F_m) by the transfer of one electron (Fig. 8A, 10 s dark interval). The longer the dark interval the more PQH_2 becomes oxidized, resulting in lower level of the J inflection.

Thus, partial pre-reduction of PQ and Q_A in dark-adapted objects truncates the initial part of FI curves, leading to misinterpretation of excitonic connectivity. In leaves the typical F_m/F_0 ratio is about ten (PSI fluorescence subtracted). Smaller ratios are warning about significant pre-reduction of Q_A.

Donor side quenching

Most researchers have been reluctant to identify the number of quenched excitations with the number of separated charges, i.e., to assume that charge separation is the only excitation quenching process (as long as non-photochemical quenching in the antenna is absent). We disregarded these warnings and calculated the "complementary area" (the cumulative number of excitations quenched by PSII, n_q), expecting to see whether its kinetic properties would suggest a solution for the long-lasting problem of the donor side quenching of fluorescence. The approach suggests a mechanism based on charge separation indeed, therefore, we may abandon the term "excitations quenched by PSII", and identify these with the number of charges separated by PSII.

Recently we investigated oxygen evolution and chlorophyll fluorescence induced by multiple turnover light pulses of various length and intensity in sunflower leaves (Oja et al. 2011; Laisk et al. 2012). In interpretation we proceeded from the "six-pack" model of excitonically coupled donor side pigments (Renger 2010), according to which P680 is just a spectroscopic term for an excited state of a pigment complex, $P680^* = (P_{D1}P_{D2}Chl_{D1}Chl_{D2}Pheo_{D1}\text{-}Pheo_{D2})^*$. Fluorescence is emitted at the F_m level if charge cannot be separated from any of the components of the six-pack. Fluorescence is quenched close to the F_0 level as a result of electron departure to Q_A from any of the components, but most likely from Chl_{D1} and $Pheo_{D1}$, terminating excitonic reversibility between P680* and the antenna. We found that at high excitation rates the actual electron transport rate detected from O_2 evolution was much lower than the rate of charge separation, calculated from photochemical fluorescence quenching.

Such a difference between fluorescence quenching and actual PSII electron transport is known as the donor side quenching, assumed to be caused by a non-photochemical quencher, not related to charge separation, or by recombination of separated charges (Schreiber 2002). Our experiments of Fig. 10 show that the donor side quenching is interfering with fluorescence interpretation even earlier than usually believed. Assuming that the donor side quenching was absent at a PFD of 250 μmol m^{-2} s^{-1}, 8 % excitations were donor side quenched at 500, 17 % at 1,000, and 31 % at PFD of 3,000 μmol m^{-2} s^{-1}. This warns about significant overestimation of PSII electron transport by the PEA fluorometer, usually operated at the latter actinic beam intensity. Suggested candidates for such a non-photochemical quencher were listed in the Introduction (Stirbet and Govindjee 2012), the most popular one being $P680^+$. However, it is established now that $P680^+$ is rapidly (generally faster than 1 μs, Reifarth et al. 1997; Christen et al. 1998) re-reduced by electron transfer from TyrZ, leaving $TyrZ^{ox}$ to be the long-living positive hole on the donor side. In accordance with this, $P680^+$ levels are undetectably low in intact leaves even under very high excitation rates (Laisk et al. 2012). The problem with $TyrZ^{ox}$ is, it is not known to possess properties of non-photochemical excitation quenching. Nevertheless, it is the only compound on the donor side, suitably oxidized for participation in the donor side quenching. For this reason we still propose that charge separation in connection with $TyrZ^{ox}$ must be involved as the principal excitation quencher process.

The major unsolved enigma of PSII fluorescence analysis is the third level of fluorescence yield—neither F_0 nor

F_m, but the level of about 0.5 F_m or slightly higher is observed after flashing with a SSTF (Mauzerall 1972; Schreiber 1986; Schreiber et al. 1995; Samson and Bruce 1996). This same level of fluorescence is actually approached as the maximum level of the J inflection, when the excitation light is increased to very high values (Kobližek et al. 2001). There is no doubt that Q_A is completely reduced immediately after a SSTF, but fluorescence yield is still significantly lower than F_m. This fact has forced investigators to assume that a non-photochemical quencher is generated by the high excitation light, which—for an unknown reason—disappears while fluorescence is approaching F_m during the thermal phase. According to this model, the thermal phase is not caused by continuing Q_A reduction during electron transport through the two photosystems, but is a result of not yet known processes removing the donor side quenching, e.g. conformational changes in proteins (Schansker et al. 2013).

Let us recall that the donor side quencher appears only at high excitation rates, causing the quenching of about 30 % excitations at PFD of 3,000 μmol m^{-2} s^{-1} (Fig. 10), but even more at higher PFDs. Such response suggests that—like the dead time in the Geiger–Müller counter of nuclear particles—the quencher, having a certain life-time, is created after each successful electron transfer. At low light intensities the next photon seldom hits a PSII with the quencher still alive, but at 3,000 μmol quanta m^{-2} s^{-1} about 30 % of photons hit a PSII where the quencher, created by a preceding charge separation, is still active.

At this point it seems to be an inevitable assumption that the quencher is $TyrZ^{ox}$. $TyrZ^{ox}$ is formed after a successful charge transfer to Q_A in a PSII having donor side reduced and acceptor side oxidized, but is not generated in PSII where Q_A and TyrZ both are reduced—what happens with the accumulation of PQH_2. Thus, the true F_m level can be achieved only together with the complete reduction of PQ, fully blocking electron transport through PSII and prohibiting the oxidation of TyrZ. As long as electron transport through a fraction of PSII is still possible, TyrZ becomes oxidized and the next photon may be donor side quenched in these PSII.

If $TyrZ^{ox}$ is the quencher, its life-time is determined by the rate of S-state advancement. Our analysis of Fig. 11 revealed a value of 0.42 ms for the average donor side quencher life-time, which is in reasonable agreement with the estimated average over S-states time of $TyrZ^{ox}$ re-reduction by WOC: the half-times found for electron transfer (at pH 6.5) were 250 μs for $Y_Z^+S_0 \rightarrow Y_ZS_1$, 55 μs for $Y_Z^+S_1 \rightarrow Y_ZS_2$ $Y_Z^+S_1 \rightarrow Y_ZS_2$, 290 μs for $Y_Z^+S_2 \rightarrow Y_ZS_3$, and 1.2 ms for $Y_Z^+S_3 \rightarrow Y_ZS_0$ (Rappaport et al. 1994), the average being 0.45 ms.

In our experimental framework the mechanism of excitation quenching by $TyrZ^{ox}$ can only be suggested as a hypothesis. Since there is no evidence about its non-photochemical activity, we have to assume that $TyrZ^{ox}$ quenches excitation photochemically—being an electron acceptor from the excited pigment complex P680*. The proposed logic of the donor side quenching thus is the following. Whatever the illumination pattern (including SSTF), the first photon hitting a PSII with reduced TyrZ and P680 and oxidized Q_A performs electron transfer to Q_A. The rate constant for this electron transfer is about nine times faster than the rate constant for intrinsic excitation conversion to fluorescence and heat in the antenna—meaning that for the first hit the F_0 level is about 1/10 of the F_m level. The formed $P680^+$ is rapidly (mostly within 1 μs) reduced, leaving $TyrZ^{ox}$ on the donor side and Q_A^- on the acceptor side. The lifetime of both, $TyrZ^{ox}$ and Q_A^-, is roughly equal, between 0.2 and 0.6 ms for the most S-states (Rappaport et al. 1994; de Wijn and van Gorkom 2001). If another photon hits a PSII in this state, P680 becomes excited, but charge transfer to Q_A^- is not possible. Instead, there is another oxidized quinone-like compound at a distance of 8.4 Å—$TyrZ^{ox}$. We suggest (see also Laisk et al. 2012) that charge transfer occurs between P680* and $TyrZ^{ox}$, more specifically between the excited Chl_{D1} and $TyrZ^{ox}$. The rate constant for this charge transfer is still significantly slower than that to Q_A, because the resulting fluorescence quenching is not for ten times, but by about a half—it is the fluorescene level recorded after excitation by SSTF, or the typical J inflection level during very strong illumination. In the normal direction ($TyrZ \rightarrow P680^+$) such electron transfer occurs faster than within a microsecond at each successful charge transfer. In the reverse direction ($P680^* \rightarrow TyrZ^{ox}$) this transfer may be faster due to the larger free energy gap. Such an electron transfer is possible indeed, as judged by the tunneling distance between Chl_{D1} and TyrZ, but a problem may arise due to the too large free energy gap (Moser et al. 2005), creating difficulties for thermal dissipation of energy (except if the reorganization energy of the product happens to be very large). At least with a closed reaction center the conversion of antenna Chl* excitation to heat occurs with a life-time of a few ns (the life-time of F_m), despite the free energy change being about as large as that associated with electron transfer from P680* to $TyrZ^{ox}$. If the rate constant for electron transfer ($P680^*$ $TyrZ^{ox}$) → ($P680^+$ TyrZ + heat) is also about $(2\ ns)^{-1}$, comparable to that of intrinsic de-excitation ($P680^* \rightarrow P680$ + heat), the two rates in parallel will result in the fluorescence yield of 0.5 F_m.

This hypothetical mechanism thus predicts a third value of fluorescence yield between F_m and F_0, which we denote F_f (from "flash"). After each charge separation the donor side quenching lasts as long as TyrZ remains oxidized and Q_A reduced. In DCMU-poisoned objects Q_A remains reduced for

long time, therefore, in these objects the F_f level is reached immediately after the flash, but later the fluorescence yield increases, approaching F_m as fast as $TyrZ^{ox}$ becomes re-reduced (e.g., during about 0.5 ms, Schreiber 2002). This fact clearly distinguishes the $TyrZ^{ox}$ based model of donor side quenching from the model based on charge recombination from Q_B, which should disappear in the presence of DCMU (Schreiber 2002). In non-inhibited objects the SSTF-induced fluorescence immediately reaches the F_f level, but then decreases, approaching F_0 with complex kinetics (de Wijn and van Gorkom 2001; De Wijn et al. 2001; Schreiber 2002). This shows that, on average, Q_A is mostly oxidized faster than $TyrZ^{ox}$ becomes reduced, avoiding the transient state of F_m, with both TyrZ and Q_A reduced.

What happens when a photon hits the transient state with both TyrZ and Q_A oxidized, is difficult to say. Our experiments with double SSTFs showed that the O_2 production efficiency of the second flash of a pair restored with two exponential time constants of 0.25 and 0.9 ms between the flashes (Oja et al. 2011), indicating that double advancement of S-states in response to two photons, the second arriving while TyrZ was oxidized, did not occur. Thus, the possibility of electron transfer to Q_A from the state $TyrZ^{ox}$ P680*Q_A is unlikely, but cycling via $TyrZ^{ox}$ is still preferred, e.g., because of the high local electric field restricting the transfer of two electrons through the membrane, leaving two holes on the donor side. The suggested pathway of $TyrZ^{ox}$ reduction by P680* does not compete with the ordinary Q_A reduction process, because electron transfer from P680* to Q_A is much faster (hundreds of ps) than the oxidation of TyrZ (up to a μs), so that TyrZ remains reduced during electron transfer to Q_A.

In the light of these experiments the second quencher in the double-hit process of Joliot and Joliot (1977) is $TyrZ^{ox}$, which is photochemically reduced by electron transfer from P680*, most likely from Chl_{D1}. In fact the quenching process is not double-hit limited, but the quencher is effective during about 0.4 ms after each successful charge separation, being able to carry out dissipative cyclic electron transfer with charge transfer rate constant sufficiently fast to quench the fluorescence yield down to about 0.5 F_m, the typical fluorescence yield, F_f, after SSTF excitation. For example, during a xenon SSTF excitations arrive after about 1 μs. The estimated charge transfer time to TyrZ of a few ns and cycling back from TyrZ to $P680^+$ of 1 μs allow electron cycling via the route P680* → TyrZ → P680 → P680* fast enough to quench excitation even during a SSTF (complemented by singlet–triplet annihilation at such high intensities).

The later phases of the multiphase FI transient are explainable by dynamics of Q_A reduction, which is reduced by light at the maximum rate allowed by S-state advancement, but simultaneously oxidized by electron transfer to Q_B, further to PQ and via Cyt b_6f to PSI and further to its acceptor side carriers. The strong re-binding of PQH_2 inhibits PSII electron transport proportionally with the PQ reduction level. As soon as the increasing Q_A reduction begins to restrict electron flow, TyrZ no longer becomes oxidized and the donor side quenching disappears. The FI transient of Fig. 10, plotted against the number of quenched excitations (=transferred electrons), clearly exhibits the J inflection (0.5 F_m at n_q of 1–2 e^- per PSII, PFD of 3,000 μmol m^{-2} s^{-1}), I inflection (0.8F_m at n_q of 7 e^- per PSII) and P peak (at 19 e^- per PSII). At this relatively high PFD a large part of Q_A may be reduced at the J inflection, but fluorescence is quenched by TyrZ as explained above. During the J–I phase electron transfer rate through Cyt b_6f is constant (driven by PSI, saturated by PQH_2), but lower than electron arrival rate into PQ through PSII at this PFD. As a result of this PQ becomes gradually more reduced, closing the acceptor side of a proportional fraction of PSII. At the I inflection the rates of electron arrival and departure become equal in the PQ pool, electron transport continues at a constant rate supported by PSI (and PSII) until the pools become reduced at the acceptor and donor side of PSII (about 15–7 = 12 e^- per PSII). The transient is completed by the full reduction of PQ (the final phase between 15 and 19 e^- per PSII). At low light (250 μmol m^{-2} s^{-1}) the I inflection is missing, because electron supply into the PQ pool by PSII is slower than consumption by PSI. At the low light the pool sizes of electrons in PQ and around PSI are kinetically segregated even better than at the high light. The horizontal part of the low light trace represents electron transport through PSI at a constant rate limited by PSII light intensity (about 10–11 e^- per PSII). The final sloped part is associated with PQ reduction after PSI electron transport stopped (about 6 e^- per PSII). This example shows the benefits of plotting the FI trace against the number of quenched photons—the x-axis value at the characteristic inflections is just equal to the number of transferred electrons.

Acknowledgments This work was supported by Targeted Financing Theme SF0180045s08 from Estonian Ministry of Education and Science and Grants 8283 and 8344 from Estonian Science Foundation. Contribution by reviewers, whose constructive criticism helped to finish the statements to their final clarity, is highly appreciated.

Appendix

Excitonic connectivity in a domain of several PSII centers. A mathematical model for the DCMU-inhibited case

This model describes the induction of fluorescence, as the number of closed centers with reduced Q_A, n, increases, in

a domain containing N PSII centers having a common antenna. Photochemical excitation capture rate constant from the antenna is assumed to be proportional with the number of open centers, N—n. In terms of rate constants of excitation capture, fluorescence yield as a function of reduced centers, n, is

$$F_n = \frac{k_f}{k_f + k_n + (N-n)k_\mathrm{p}}, \tag{5}$$

and

$$F_\mathrm{m} = \frac{k_f}{k_f + k_n} \tag{6}$$

Here rate constants k stand for (subscripts) f, fluorescence emission, n, non-photochemical quenching and p, photochemistry. Correspondingly

$$\frac{F_n}{F_\mathrm{m}} = \frac{k_f + k_n}{k_f + k_n + (N-n)k_\mathrm{p}} = \frac{1}{1 + \frac{k_\mathrm{p}}{k_f + k_n}(N-n)} \tag{7}$$

When all centers are open then fluorescence is F_0:

$$\frac{F_0}{F_m} = \frac{1}{1 + \frac{k_\mathrm{p}}{k_f + k_n}N} \quad \text{or} \quad \frac{F_\mathrm{m}}{F_0} = 1 + \frac{k_\mathrm{p}}{k_f + k_n}N$$

from where

$$\frac{k_\mathrm{p}}{k_f + k_n} = \frac{\frac{F_\mathrm{m}}{F_0} - 1}{N}. \tag{8}$$

Inserting (8) into (7) we obtain a formula relating the fluorescence yield of a domain with n reduced centers to the maximum fluorescence F_m and minimum fluorescence F_0:

$$\frac{F_n}{F_\mathrm{m}} = \frac{NF_0}{(N-n)F_\mathrm{m} + nF_0} \tag{9}$$

Denoting B_n the fraction of domains with n reduced centers, the following differential equations describe the advancement of B_n with illumination from $n = 0$ to $n = N$, beginning with $B_0 = 1$, $B_1 \ldots B_\mathrm{N} = 0$ and ending with $B_0 \ldots B_{\mathrm{N}-1} = 0$, $B_\mathrm{N} = 1$:

$$\mathrm{d}B_0 = -\left(1 - \frac{F_0}{F_\mathrm{m}}\right)B_0 \cdot \mathrm{d}q \tag{10}$$

$$dB_\mathrm{n} = \left[\left(1 - \frac{F_{\mathrm{n}-1}}{F_\mathrm{m}}\right)B_{\mathrm{n}-1} - \left(1 - \frac{F_\mathrm{n}}{F_\mathrm{m}}\right)B_\mathrm{n}\right] \cdot dq \tag{11}$$

$$\mathrm{d}B_\mathrm{N} = \left(1 - \frac{F_{N-1}}{F_\mathrm{m}}\right)B_{N-1} \cdot \mathrm{d}q \tag{12}$$

For the DCMU-inhibited case we neglect the re-oxidation of Q_A, once reduced. In Eqs. (10, 11, 12, 13) dq stands for cumulative excitation of the whole domain:

$$\mathrm{d}q = N\frac{a_\mathrm{II}}{N_\mathrm{PSII}}I(t)\mathrm{d}t, \tag{13}$$

where $I(t)$ is PAD by the leaf, a_II is excitation partitioning to PSII and N_PSII is PSII density per area unit. The formula is a development of Eq. (1) in the main text, but multiplied by N, the number of individual PSII centers in the domain.Fluorescence of the whole leaf is the sum of all fractions,

$$\frac{F}{F_\mathrm{m}} = \sum_{n=0}^{N}\frac{F_n}{F_\mathrm{m}}B_n, \tag{14}$$

but Q_A reduction is

$$Q_\mathrm{A} = \frac{1}{N}\sum_{n=0}^{N} nB_n. \tag{15}$$

Assuming that each quenched excitation (the abscissa of Fig. 4) performs Q_A reduction, the theoretical curve in Fig. 5 is a plot of Eqs. (14) versus (15), the best fit to experimental data obtained with $N = 4$.

References

Broess K, Trinkunas G, van der Wej-de Wit SD, Dekker JP, van Hock A, van Amerongen H (2006) Excitation energy transfer and charge separation in photosystem II membranes revisited. Biophys J 91:3776–3786

Broess K, Trinkunas G, van Hoek A, Croce R, van Amerongen H (2008) Determination of the excitation migration time in photosystem II—consequences for the membrane organization and charge separation parameters. Biochim Biophys Acta 1777:404–409

Cafarri S, Broess K, Croce R, van Amerongen H (2011) Excitation energy transfer and trapping in higher plant photosystem II complexes with different antenna sizes. Biophys J 100:2094–2103

Canaani O, Malkin S (1984) Distribution of light excitation in an intact leaf between the two photosystems of photosynthesis. Changes in absorption creoss-sections following State1–State2 transitions. Biochim Biophys Acta 766:512–524

Chow WS, Hope AB, Anderson JM (1991) Further studies on quantifying photosystem 2 in vivo by flash-induced oxygen yield from leaf discs. Aust J Plant Physiol 18:397–410

Christen G, Reifarth F, Renger G (1998) On the origin of the '35-μs kinetics' of $P680^{+\bullet}$ reduction in photosystem II with an intact water oxidizing complex. FEBS Lett 429:49–52

de Wijn R, van Gorkom HJ (2001) Kinetics of electron transfer from Q_A to Q_B in photosystem II. Biochemistry 40:11912–11922

de Wijn R, Schrama T, van Gorkom HJ (2001) Secondary stabilization reactions and proton-coupled electron transport in photosystem II investigated by electroluminescence and fluorescence spectroscopy. Biochemistry 40:5821–5834

Delosme R (1967) Étude de l'induction de fluorescence des algues vertes et des chloroplastes an début d'une illumination intense. Biochim Biophys Acta 143:108–128

den Hollander WTF, Bakker JGC, van Grondelle R (1983) Trapping, loss and annihilation of excitations in a photosynthetic systemI. I. Theoretical aspects. Biochem Biophys Acta 725:492–507

Duysens LNM, Sweers HE (1963) Mechanisms of two photochemical reactions in algae as studied by means of fluorescence. In: Japanese Society of Plant Physiologists, studies on microalgae and photosynthetic bacteria, Special Issue of Plant and Cell Physiology. University of Tokyo Press, Tokyo, p 353–372

Franck F, Juneau P, Popovic R (2002) Resolution of the photosystem I and photosystem II contributions to chlorophyll fluorescence of intact leaves at room temperature. Biochim Biophys Acta 1556:239–246

Genty B, Wonders J, Baker NR (1990) Non-photochemical quenching of F0 in leaves is emission wavelength dependent: consequences for quenching analysis and its interpretation. Photosynth Res 26:133–139

Haferkamp S, Haase W, Pascal AA, van Amerongen H, Kirchhoff H (2010) Efficient light harvesting by photosystem II requires an optimized protein packing density in grana thylakoids. J Biol Chem 285:17020–17028

Han G, Mamedov F, Styring S (2012) Misses during water oxidation in photosystem II are state dependent. J Biol Chem 287:13422–13429

Hankamer B, Morris E, Zheleva D, Barber J (1995) Biochemical characterization and structural analysis of monomeric and dimeric photosystem II core preparations. In: Mathis P (ed) Photosynthesis: from light to biosphere, vol III. Kluwer Academic Publishers, Dordrecht, pp 365–367

Hogewoning SW, Wientjes E, Douwstra P, Trouwborst G, van Ieperen W, Croce R, Harbinson J (2012) Photosynthetic quantum yield dynamics: from photosystems to leaves. Plant Cell 24:1921–1935

Jans F, Mignolet E, Houyoux P-A, Cardol P, Ghysels B, Cuine S, Cournac L, Peltier G, Remacle C, Franck F (2008) A type II NAD(P)H dehydrogenase mediates light-independent plastoquinone reduction in the chloroplast of *Chlamydomonas*. PNAS 105:20546–20551

Joliot A, Joliot P (1964) Étude cinétique de la réaction photochimique libérant l'oxygène au cours de la photosynthése. C R Acad Sc Paris 258:4622–4625

Joliot P, Joliot A (1977) Evidence for a double hit process in photosystem II based on fluorescence studies. Biochim Biophys Acta 462:559–574

Joliot P, Joliot A (1979) Comparative study of the fluorescence yield and of the C550 absorption change at room temperature. Biochim Biophys Acta 546:93–105

Joliot P, Joliot A (1981) Double photoreactions induced by laser flash as measured by oxygen emission. Biochim Biophys Acta 638:132–140

Joliot P, Joliot A (1992) Electron transfer between photosystem II and the cytochrome b/f complex: mechanistic and structural implications. Biochim Biophys Acta 1102:53–61

Joliot P, Joliot A (2002) Cyclic electron transfer in plant leaf. PNAS 99:10209–10214

Joliot P, Joliot A (2003) Excitation transfer between photosynthetic units: the 1964 experiment. Photosynth Res 76:241–245

Joliot P, Bennoun P, Joliot A (1973) New evidence supporting energy transfer between photosynthetic units. Biochim Biophys Acta 305:317–328

Joliot P, Lavergne J, Béal D (1992) Plastoquinone compartmentation in chloroplasts. I. Evidence for domains with different rates of photo-reduction. Biochim Biophys Acta 1101:1–12

Kobližek M, Kaftan D, Nedbal L (2001) On the relationship between the non-photochemical quenching of the chlorophyll fluorescence and the photosystem II light harvesting efficiency. A repetitive flash fluorescence induction study. Photosynth Res 68:141–152

Kramer DM, Johnson G, Kiirats O, Edwards GE (2004) New fluorescence parameters for the determination of Q_A redox state and excitation energy fluxes. Photosynth Res 79:209–218

Laisk A, Nedbal L, Govindjee (2009) Photosynthesis in Silico. Undestanding complexity from molecules to ecosystems. Springer, Dordrecht

Laisk A, Eichelmann H, Oja V (2012) Oxygen evolution and chlorophyll fluorescence from multiple turnover light pulses: charge recombination in photosystem II in sunflower leaves. Photosynth Res 113:145–155

Laureau C, De Paepe R, Latouche G, Moreno-Chacon M, Finazzi G, Kunz M, Cornic G, Streb P (2013) Plastid terminal oxidase (PTOX) has the potential to act as a safety valve for excess excitation energy in the alpine plant species *Ranunculus glacialis* L. Plant Cell Env 36:1296–1310

Lavergne J, Bouchaud J-P, Joliot P (1992) Plastoquinone compartmentation in chloroplasts. II. Theoretical aspects. Biochim Biophys Acta 1101:13–22

Malkin S, Kok B (1966) Fluorescence induction studies in isolated chloroplasts. I-Number of components involved in the reaction and quantum yields. Biochim Biophys Acta 126:413–432

Mauzerall D (1972) Light-induced fluorescence changes in Chlorella, and the primary photoreactions for the production of oxygen. Proc Natl Acad Sci USA 69:1358–1362

Melis A, Homann PH (1975) Kinetic analysis of fluorescence induction in 3-(3,4-dichlorophenyl)-1,1-dimethylurea poisoned chloroplasts. Photochem Photobiol 21:431–437

Morin P (1964) Études des cinétiques de fluorescence de la chlorophylle in vivo, dans les premiers instants qui suivent le début de l'illumination. J Chem Phys 61:674–680

Moser CC, Page CC, Dutton PL (2005) Tunneling in PSII. Photochem Photobiol Sci 4:933–939

Neubauer C, Schreiber U (1987) The polyphasic rise of chlorophyll fluorescence upon onset of strong continuous illumination: I. Saturation characteristics and partial control by the photosystem II acceptor side. Z Naturforschung 42c:123–131

Oja V, Laisk A (2000) Oxygen yield from single turnover flashes in leaves:non-photochemical excitation quenching and the number of active PSII. Biochim Biophys Acta 1460:291–301

Oja V, Laisk A (2012) Photosystem II antennae are not energetically connected: evidence based on flash-induced O_2 evolution and chlorophyll fluorescence in sunflower leaves. Photosynth Res 114:15–28

Oja V, Eichelmann H, Anijalg A, Rämma H, Laisk A (2010) Equilibrium or disequilibrium? A dual-wavelength investigation of photosystem I donors. Photosynth Res 103:153–166

Oja V, Eichelmann H, Laisk A (2011) Oxygen evolution from single- and multiple-turnover light pulses: temporal kinetics of electron transport through PSII in sunflower leaves. Photosynth Res 110:99–109

Paillotin G (1976) Movement of excitations in the photosynthetic domains of photosystem II. J Theor Biol 58:237–252

Palombi L, Cecchi G, Lognoli D, Raimondi V, Toci G, Agati G (2011) A retrieval algorithm to evaluate the photosystem I and photosystem II spectral contributions to leaf chlorophyll fluorescence at physiological temperatures. Photosynth Res 108:225–239

Peterson R, Oja V, Laisk A (2001) Chlorophyll fluorescence at 680 and 730 nm and its relationship to photosynthesis. Photosynth Res 70:185–196

Pettai H, Oja V, Freiberg A, Laisk A (2005) Photosynthetic activity of far-red light in green plants. Biochim Biophys Acta 1708:311–321

Pfündel E (1998) Estimating the contribution of photosystem I to total leaf chlorophyll fluorescence. Photosynth Res 56:185–195

Rabinowitch E, Govindjee (1969) Photosynthesis. Wiley, New York

Rappaport F, Blanchard-Desce M, Lavergne J (1994) Kinetics of electron transfer and electrochromic change during the redox transitions of the photosynthetic oxygen-evolving complex. Biochim Biophys Acta 1184:178–192

Reifarth F, Christen G, Renger G (1997) Fluorimetric equipment for monitoring P_{680}^{+} reduction in PSII preparations and green leaves. Photosynth Res 51:231–242

Renger G (2010) The light reactions of photosynthesis. Curr Sci 98:1305–1319

Robinson H, Crofts AR (1983) Kinetics of the oxidation-reduction reactions of the photosystem II quinone acceptor complex, and the pathway for deactivation. FEBS Lett 153:221–226

Rumeau D, Peltier G, Cournac L (2007) Chlororespiration and cyclic electron flow around PSI during photosynthesis and plant stress response. Plant, Cell Environ 30:1041–1051

Samson G, Bruce D (1996) Origin of the low yield of chlorophyll fluorescence induced by single turnover flash in spinach thylakoids. Biochim Biophys Acta 1276:147–153

Sazanov LA, Burrows PA, Nixon PJ (1998) The chloroplast Ndh complex mediates the dark reduction of the plastoquinone pool in response to heat stress in tobacco leaves. FEBS Lett 429:115–118

Schansker G, Strasser RJ (2005) Quantification of non-Q_B-reducing centers in leaves using a far-red pre-illumination. Photosynth Res 84:145–151

Schansker G, Tóth S, Kovács L, Holzwarth AR, Garab G (2011) Evidence for a fluorescence yield change driven by a light-induced conformational change within photosystem II during the fast chlorophyll a fluorescence rise. Biochim Biophys Acta 1807:1032–1043

Schansker G, Tóth SC, Holzwarth AR, Garab G (2013) Chlorophyll a fluorescence: beyond the limits of the Q_A model. Photosynth Res. doi:10.1007/s11120-013-9806-5

Schreiber U (1986) Detection of rapid induction kinetics with new type of high-frequency modulated chlorophyll fluorometer. Photosynth Res 9:261–272

Schreiber U (2002) Assessment of maximal fluorescence yield. Donor-side dependent quenching and Q_B-quenching. In: Van Kooten O, Snel J (eds) Plant spectrophotometry: applications and basic research. Rozenberg, Amsterdam, pp 23–47

Schreiber U, Neubauer C (1987) The polyphasic rise of chlorophyll fluorescence upon onset of strong continuous illumination: II. Partial control by the photosystem II donor side and possible ways of interpretation. Z Naturforsch 42c:132–141

Schreiber U, Hormann H, Neubauer C, Klughammer C (1995) Assessment of photosystem II photochemical quantum yield by chlorophyll fluorescence quenching analysis. Aust J Plant Physiol 22:209–220

Stirbet A (2013) Excitonic connectivity between photosystem II units: What is it, and how to measure it? Photosynth Res. doi:10.1007/s11120-013-9863-9

Stirbet A, Govindjee (2012) Chlorophyll a fluorescence induction: a personal perspective of the thermal phase, the J–I–P rise. Photosynth Res 113:15–61

Strasser RJ, Butler WL (1977) Fluorescence emission spectra of photosystem I, photosystem II and the light-harvesting shloro-phyll a/b complex of higher plants. Biochim Biophys Acta 462:295–306

Strasser RJ, Govindjee (1991) The F_0 and the O-J–I–P fluorescence rise in higher plants and algae. In: Argyroudi-Akoyunoglou JH (ed) Regulation of chloroplast biogenesis. Plenum Press, New York, pp 423–426

Strasser RJ, Stirbet AD (2001) Estimation of the energetic connectivity of PSII centres using the fluorescence rise O–J–I–P. Fitting of experimental data to three different PSII models. Math Comp Simul 56:451–461

Strasser R, Tsimili-Michael M, Srivastava A (2004) Analysis of the chlorophyll a fluorescence transient. In: Papageorgiou GC, Govindjee (eds) Chlorophyll a fluorescence. A signature of photosynthesis, vol 362. Springer, Dordrecht, pp 321–362

Tóth SZ, Schansker G, Strasser RJ (2005) In intact leaves, the maximum fluorescence level (F_M) is independent of the redox state of the plastoquinone pool: a DCMU-inhibition study. Biochim Biophys Acta 1708:275–282

Tóth SZ, Schansker G, Strasser RJ (2007) A non-invasive assay of the plastoquinone pool redox state based on the OJIP-transient. Photosynth Res 93:193–203

Vredenberg VJ (2008) Algorithm for analysis of OJDIP fluorescence induction curves in terms of photo- and electrochemical events in photosystems of plant cells. Derivation and application. J Photochem Photobiol, B 91:58–65

Vredenberg W, Durchan M, Prášil O (2009) Photochemical and photoelectrochemical quenching of chlorophyll fluorescence in photosystem II. Biochim Biophys Acta 1787:1468–1478